Electronic supplementary information

In vivo X-ray spectroscopy shedding light on the mechanisms of absorption and transport of ZnO nanoparticles by plants

Tatiana N. M. da Cruz[a†], Susilaine M. Savassa[a†], Marcos H. F. Gomes[a], Eduardo dos Santos[a], Nádia M. Duran[a], Eduardo de Almeida[a], Adriana P. Martinelli[a] and Hudson W. P. de Carvalho[a*]

[a.] *Centro de Energia Nuclear na Agricultura, Universidade de São Paulo, Piracicaba, 13416-000, Brazil.*
[b.] *† These authors contributed equally to this work.*
[c.] *E-mail: hudson@cena.usp.br*

Contents

1. Estimation of the radiation dose received by the samples

To estimate the radiation dose, which the samples were submitted, besides the photon flux input, the following assumptions and approximations were made:

i) Incident energy at 9,560 eV = 1.54×10^{-15} J
ii) Time of exposure = 1,800 s, considering the time employed to adjust the sample in front of the beam
iii) Approximated mass of the irradiated volume = 4×10^{-7} kg

The absorbed radiation dose is expressed in Gray unity (Gy). Knowing that Gy = J kg^{-1}, we approximated the calculations as follows:

$$Gy = \frac{\text{number of photons per second } (s^{-1}) \times \text{time of exposure } (s) \times \text{energy of the incident photons } (J)}{\text{mass of the irradiated volume } (kg)}$$

The estimation of the radiation dose indicates that the samples received a dose lower than 1.9×10^{4} Gy.

2. Supplementary figures and tables

Fig. S1 shows a series of pictures and corresponding chemical images that uncover the spatial distribution of Zn in soybean (*Glycine max*) leaf. A 0.5 µL droplet of 2,300 mg L^{-1} $ZnSO_{4(aq)}$ was casted on the bottom side of the leaf. Then, the entire plant was placed inside of a benchtop µ-XRF equipment. The mapped area corresponds to the red rectangle shown in the pictures. The images show translocation of Zn as it is absorbed, one can clearly see Zn moving towards the main vein. Additionally, one can notice that the area that received the treatment became scorched. The foliar absorption of ions and nanoparticles have been under investigation in our group.

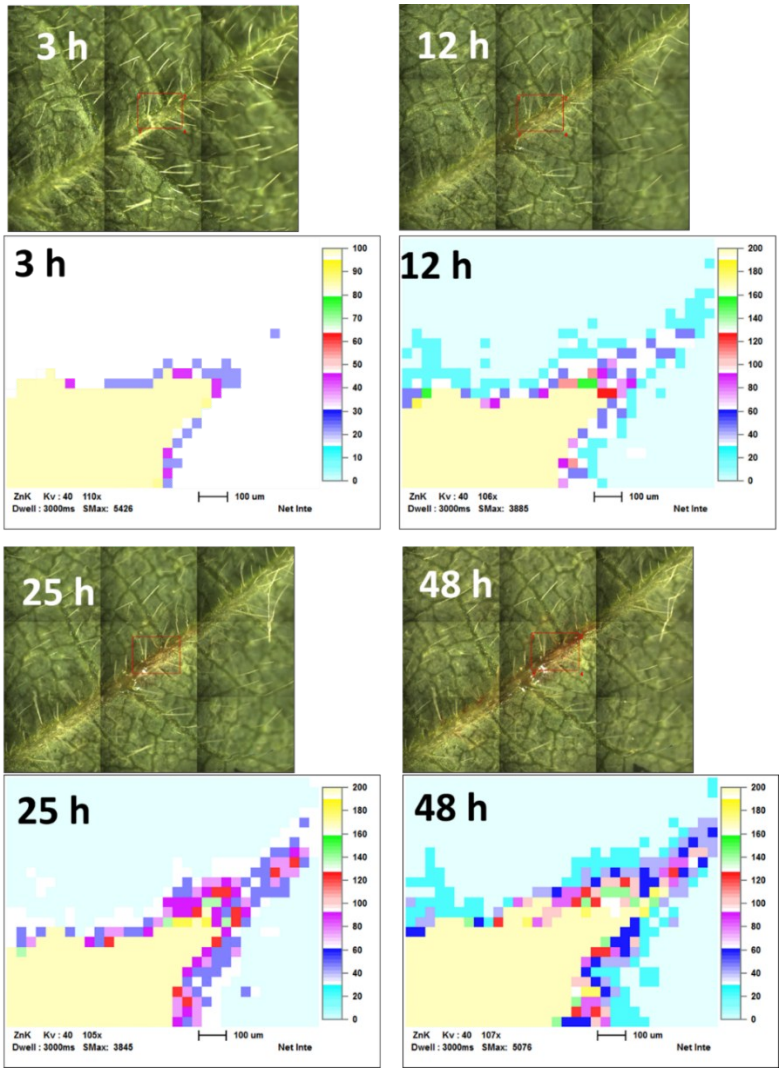

Fig. S1. Foliar Zn absorption in a soybean (*Glycine* max) leaf as function of time. A droplet of $ZnSO_{4(aq)}$ was deposited on the bottom side of the leaf and the absorption was monitored by µ-XRF.

Fig. S2 shows a plant whose roots were immersed in an aqueous dispersion of nano ZnO. The 1 mm X-ray beam, illustrated by red arrow, was shining on the stem. The Zn characteristic X-ray fluorescence, represented by the yellow arrow, was detected by SDD device. The flask containing the nano ZnO dispersion was shielded with several layers of aluminium foil to avoid any possible Zn XRF signal from the nano ZnO aqueous dispersion treatment excited by the scattered incoming beam.

Fig. S2. Setup used to monitor *in vivo* Zn uptake using a 1 mm Ø X-ray beam. The red arrow illustrates the incoming X-ray beam and the yellow one the outgoing Zn X-ray fluorescence.

The SEM images in Fig S3 show that the shape of the ZnO nanoparticles was not regular.

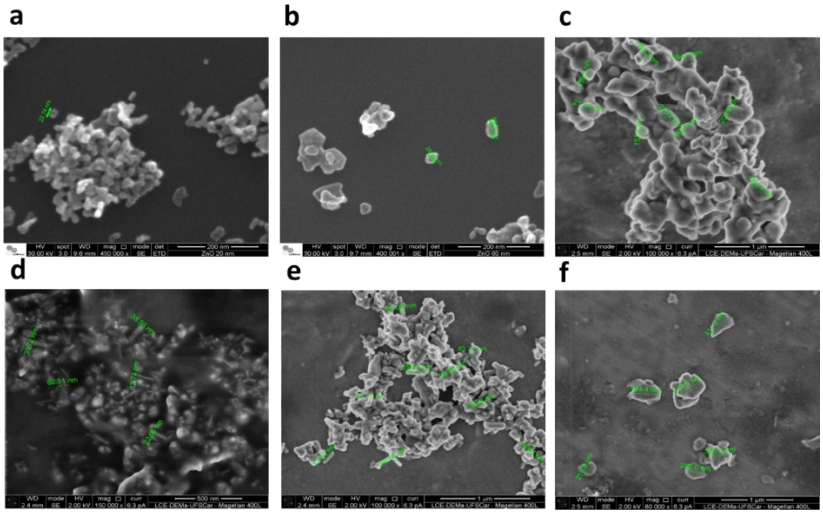

Fig. S3. Scanning electron microscopy (SEM) micrographs of ZnO nanoparticles. (a) 20 nm, (b) 40 nm and (c) 60 nm, (d) 40 nm + surfactant, (e) 60 nm + surfactant and (f) 300 nm + surfactant.

Fig. S4 presents an estimation of the solubility of nano ZnO, it also shows the recovery of $ZnSO_4$ which was above 99%. The data shows that the presence of surfactants, which identity was not disclosed by the companies, increased the solubility of the ZnO NPs only at 1,000 mg L^{-1}. The determined solubility for ZnO NP without surfactant presented values similar to the ones reported in the literature[1]. The DLS data presented in Table S1 suggests that for the 1,000 mg L^{-1} the aggregation prevention provided by the surfactant increased the particles surface exposure, therefore increasing the surface/volume ratio, which affects their solubility[2].

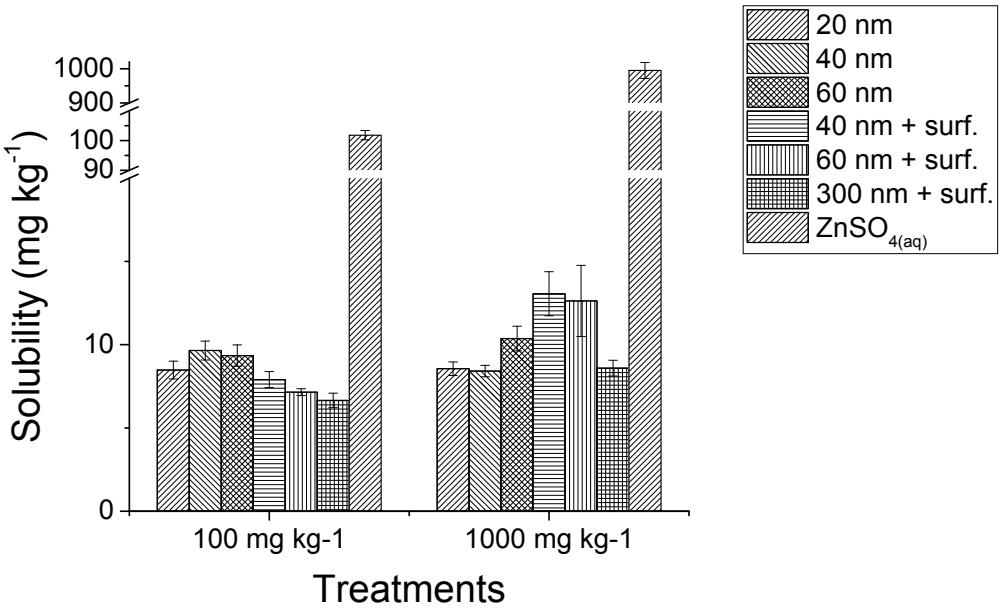

Fig S4. Solubility of nano ZnO dispersions used in the present study and recovery test for $ZnSO_{4(aq)}$.

Fig. S5 presents plots of the absorption velocity as function of the concentration of soluble Zn. In (a) is shown a log-log plot in which one can observe that points form a straight line at low concentrations of soluble Zn, *i.e*. the Zn dissolved from the ZnO nanoparticles. The plot shown in (b) did not include the $ZnSO_{4(aq)}$ points, the absorption velocity could be adjusted as an exponential function of the concentration of soluble Zn.

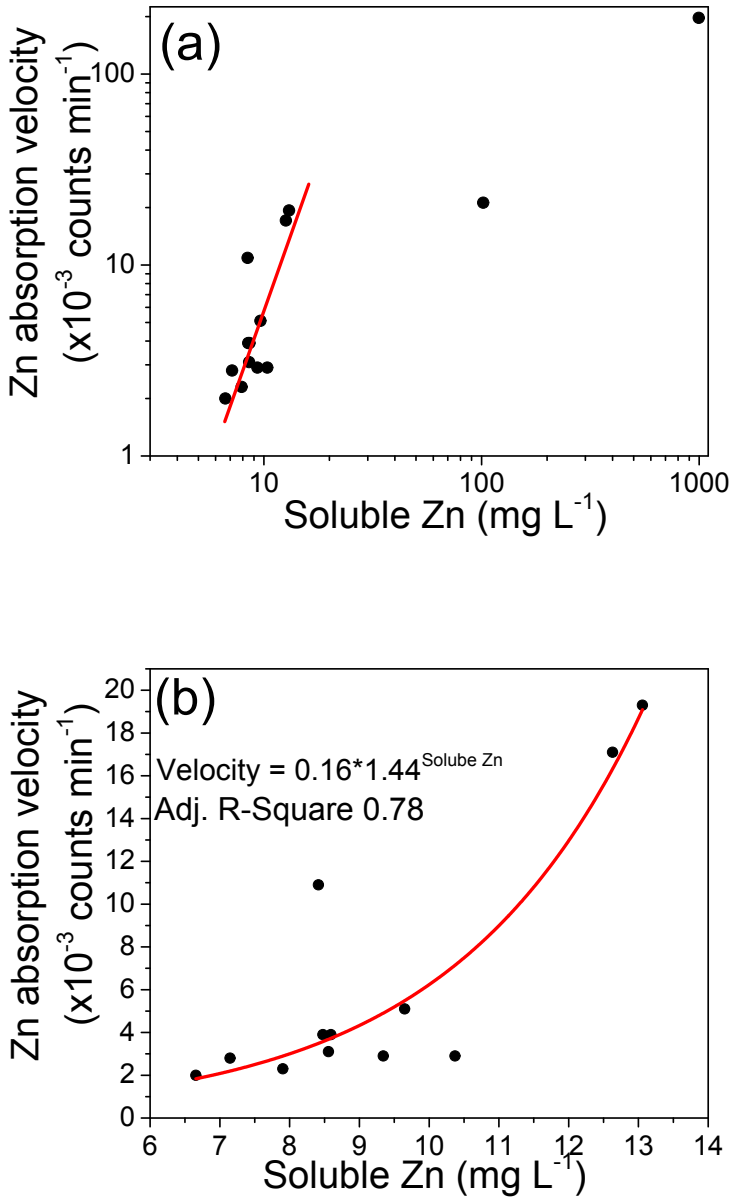

Fig. S5. (a) Log-Log uptake velocity as function of the concentration of soluble Zn; (b) uptake velocity as function of the concentration of soluble Zn released by the nanoparticles.

Fig. S6 shows scanning electron microscope micrograph of a sample equivalent to the Fig. 3 and 4 of the main manuscript, they present different stem tissues aiming to aid the interpretation of the accumulation of Zn. This image also supports the conclusion that the regions where Zn was found correspond to the vascular bundles (inner ring) and the parenchymous cells in the cortex (outer ring) (see Fig.4 of the main manuscript).

Differently from some papers, these images do not intend to locate the nanoparticles. They aim at complementing the μ-XRF chemical images.

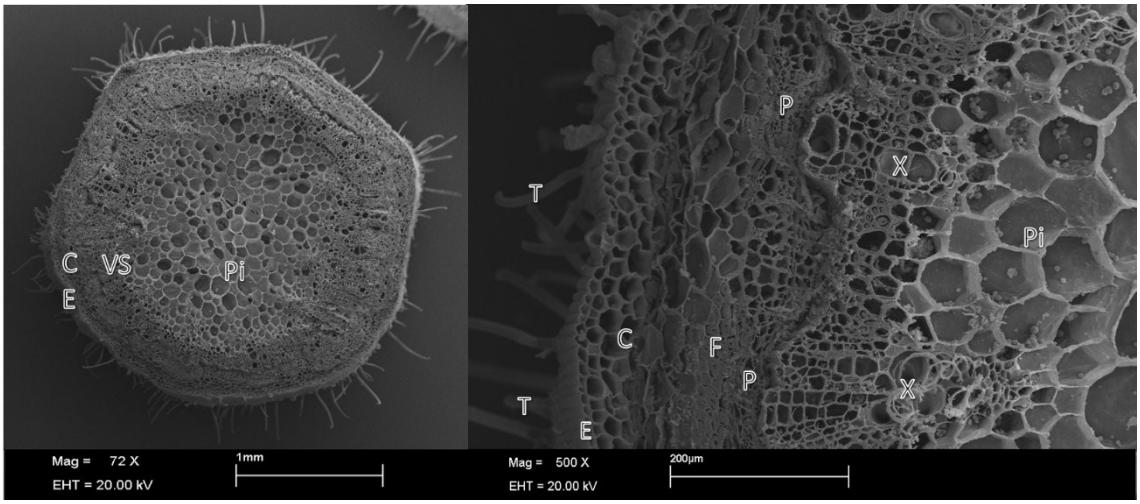

Fig. S6. Cross section of a *Phaseolus vulgaris* main stem, at 2 cm above the root crown, observed under the scanning electron microscope T= trichome, C = cortex, E = epidermis, F = fibers, Pi = Pith, P = Phloem, VS = vascular system, X = xylem.

Fig. S7 presents the same data shown in Fig. 4, except for the control sample. Nevertheless, here the intensity of Zn is plotted as 3D graph and it was also presented an overlap between the Zn maps (coloured) and Rh-Kα Compton map (black). From this perspective, one can easily observe that there is a region of lower Zn signal between two crests, which corresponds to the inner and outer ring highlighted in Fig. 4. The total number of Zn counts also increased as a function of time, in agreement with kinetics data shown in Fig. 1 and 2. Additionally, the overlapped maps show that the outer ring is close to the epidermis. The unities shown in scale corresponds net counts.

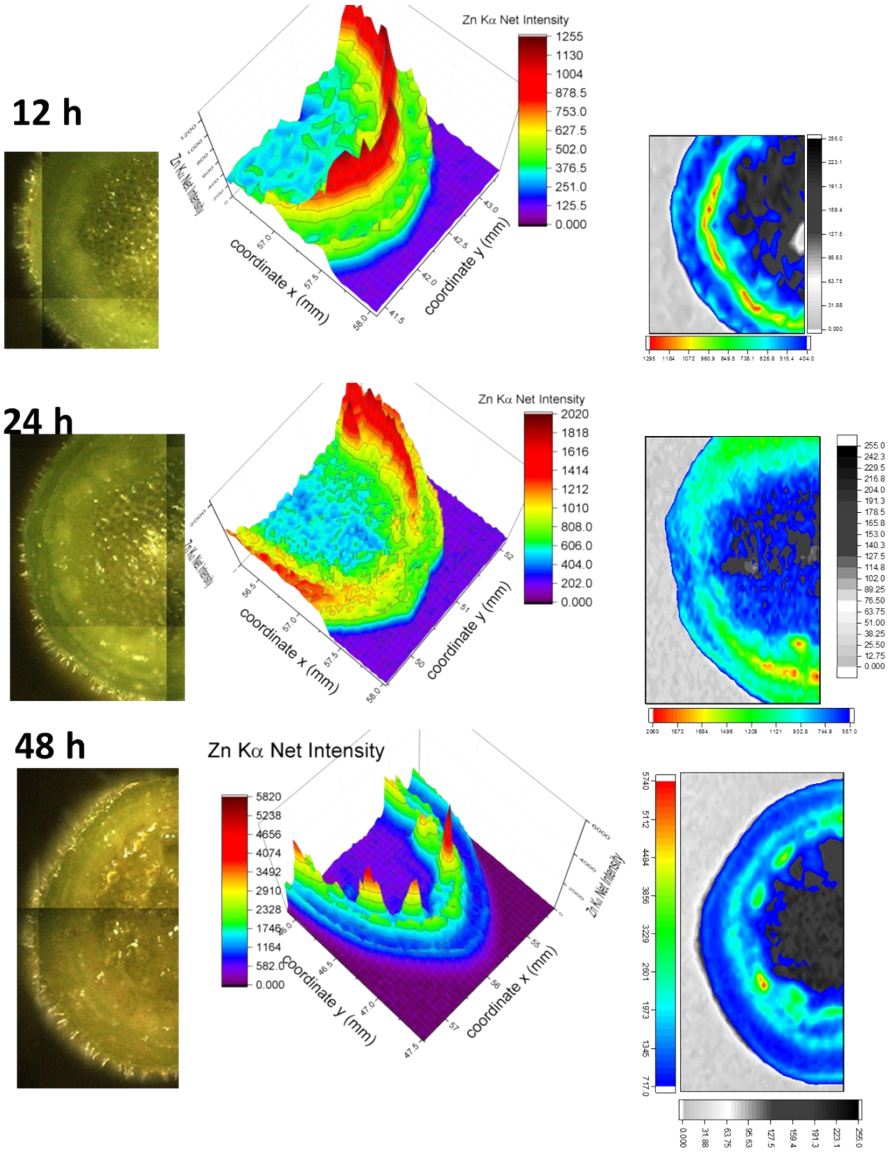

Fig. S7. 3D plots showing the spatial distribution of Zn in the stem of *Phaseolus vulgaris.* The roots of the plants exposed to 1,000 mg L^{-1} 40 nm ZnO dispersion with surfactant for 12 h, 24 h and 48 h. It is also presented overlays of XRF and Compton maps. These images correspond to the same data shown in Fig. 2 of the main manuscript.

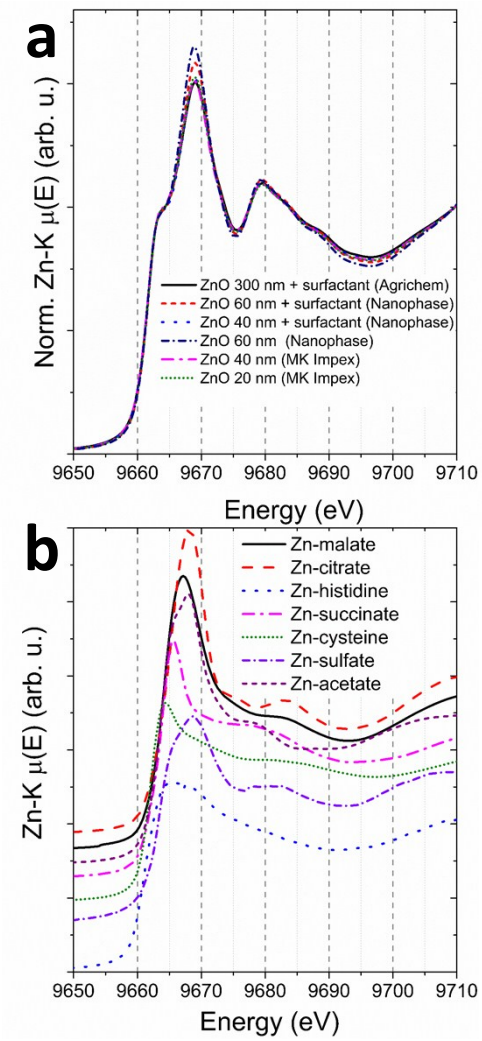

Fig. S8. (a) XANES spectra for the commercial ZnO nanomaterials employed in the present study; (b) XANES spectra for the Zn coordinate compounds synthetized in our laboratory. Since the shape of the curves are fingerprints of the chemical environment, these spectra were used in the linear combination analysis to identify the Zn forms inside of the living the plants.

Fig. S9 presents the linear combination fits for the XANES spectra *in vivo* recorded at XAFS2 beamline. The fraction of ZnO in the stem increased from (a) to (d). These measurements were performed using the setup shown in Fig. S9.

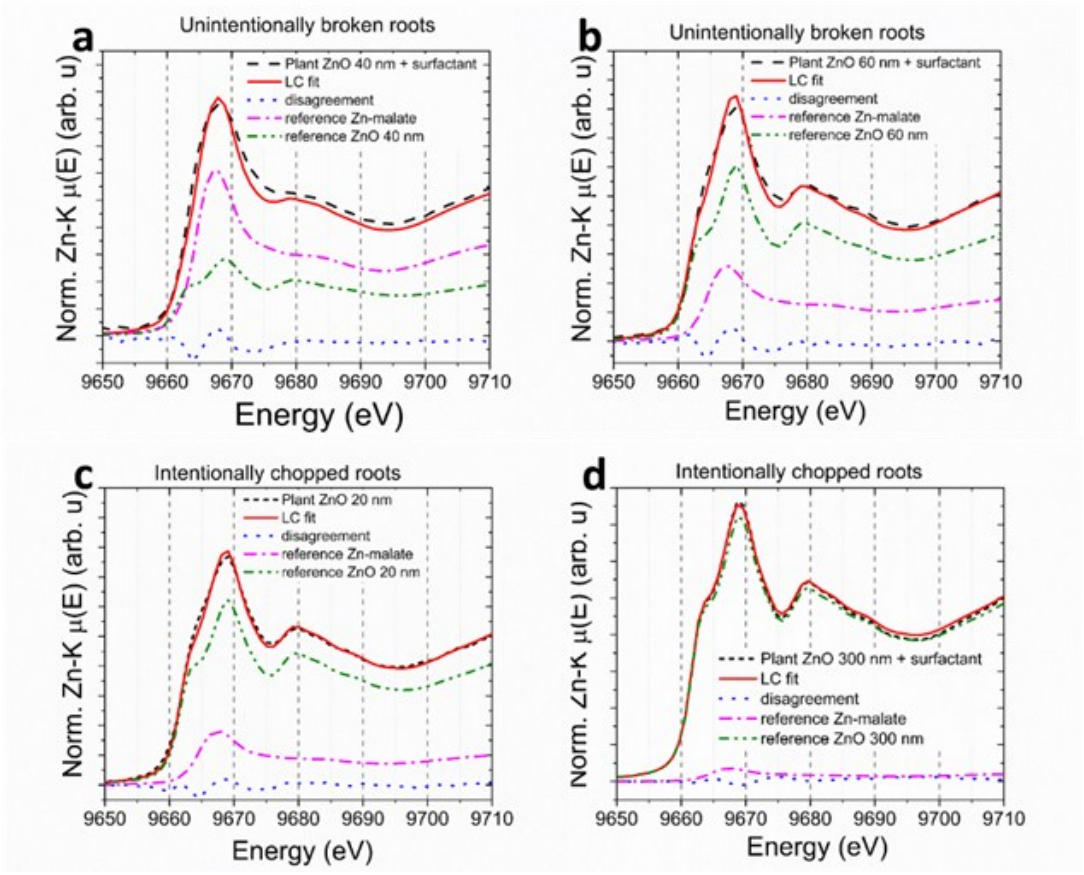

Fig. S9. Zn-K experimental XANES spectra recorded *in vivo* at the stem of *Phaseolus vulgaris* plants treated with 20, 40, 60 and 300 nm ZnO NPs, linear combination fits and the weighted spectra for the reference compounds. (a) and (b) show the spectra for plants in which exhibited damage in the roots, whereas (c) and (d) show the spectra for plants in which roots were intentionally damaged.

Fig. S10 (a) shows the roots of the sample inside of the sample holder containing the nano ZnO dispersion and (b) shows an entire plant assembled at the beamline for *in vivo* measurements at the leaf. Using this sample holder, ZnO was detected in most of the plants. However, some plants did not show ZnO. The presence of nano ZnO in the plants could not be correlated to the particle size. Nevertheless, it was associated with the damages shown in Fig. 3(c).

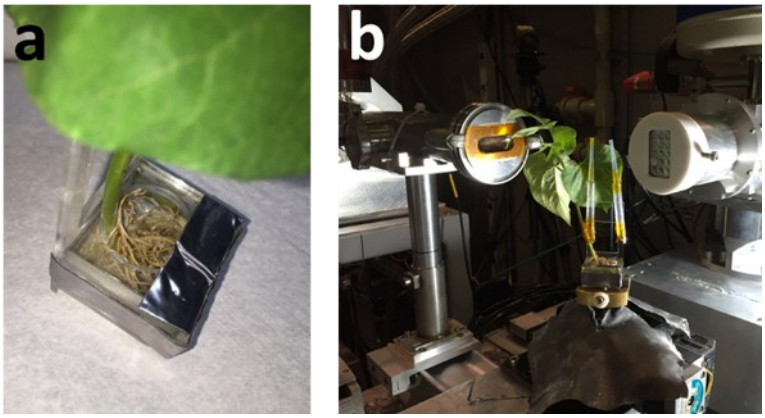

Fig S10. (a) Sample holder used to keep the roots of the bean (*Phaseolus vulgaris*) plant in contact with a dispersion of nano ZnO while recording XAS spectra in fluorescence mode; (b) Plant + sample holder assembled at XAFS2 beamline.

Fig. S11 (a) shows the setup used to record the XANES spectra for roots and (b) for stems. In this arrangement ZnO was not found in the plants. Injuries in roots were not detected as well. This has been attributed to the size of the opening of the flask in which the roots were put in contact with the nano ZnO. Since it is larger compared to Fig. S9 setup, roots were not damaged.

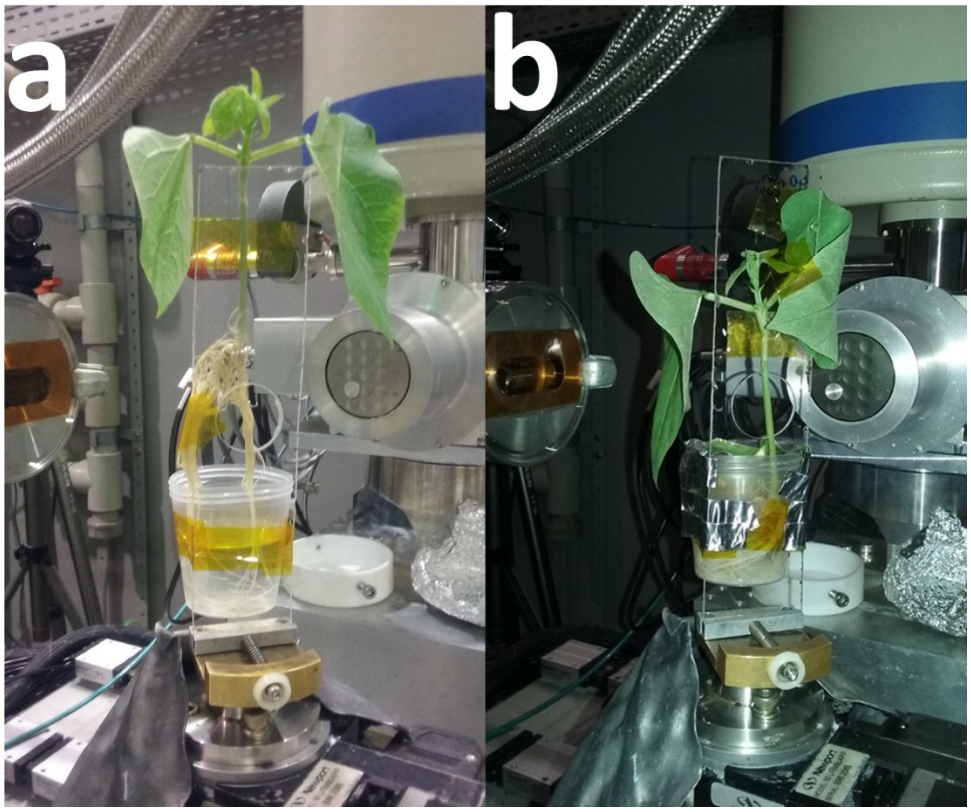

Fig. S11. Setup for recording XAS spectra in fluorescence mode for (a) root and (b) stem at XAFS2 beamline.

Fig. S12 presents the linear combination fits for the XANES spectra *in vivo* recorded at stems of the plants at XAFS2 beamline. These measurements were carried out using the setup shown in Fig. S10. In the stems of plants treated with nano ZnO without surfactant, Zn was coordinated by malate and citrate. The small fraction of citrate that improved the fit quality affected mainly the white line part of the spectra. For the plants treated with nano ZnO with surfactants, only malate was found in quantities sufficiently high to adjust the experimental spectra.

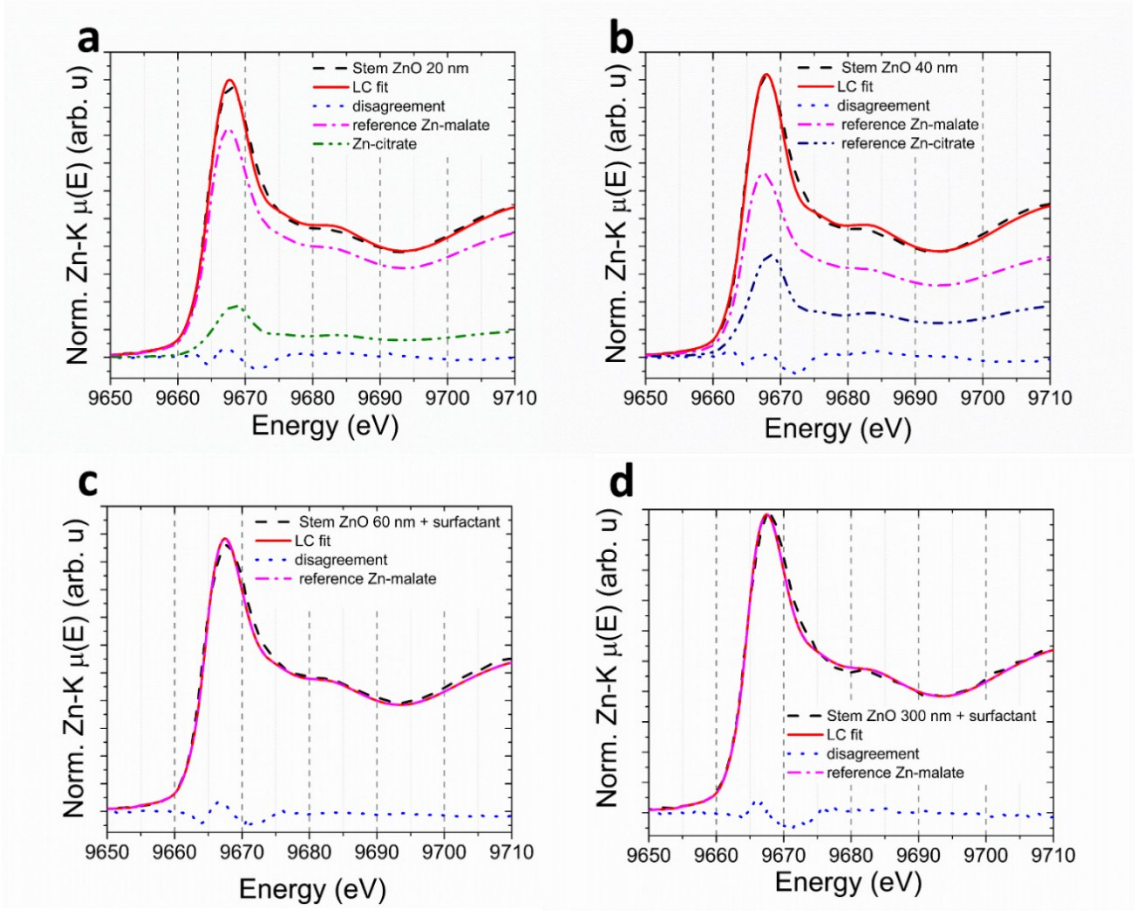

Fig. S12. Zn-K experimental XANES spectra recorded *in vivo* at the stem of bean (*Phaseolus vulgaris*) plants whose roots were immersed in nano ZnO dispersed in water; (a) 20 nm ZnO, (b) 40 nm ZnO, (c) 60 nm ZnO + surfactant and (d) 300 nm ZnO + surfactant.

Fig. S13 presents the linear combination fits for the spectra *in vivo* recorded at the roots of plants exposed to nano ZnO dispersions at the XAFS2 beamline. The fraction of citrate found was higher in roots compared to stems. The spectra for the plants treated with 40 nm ZnO (a) and with 300 nm ZnO + surfactant (d) presented also a small fraction of Zn-histidine. Zn-histidine is mainly found in leaves and according to reference[2] it corresponds to Zn stored in vacuoles. These measurements were carried out using the setup shown in Fig. S11.

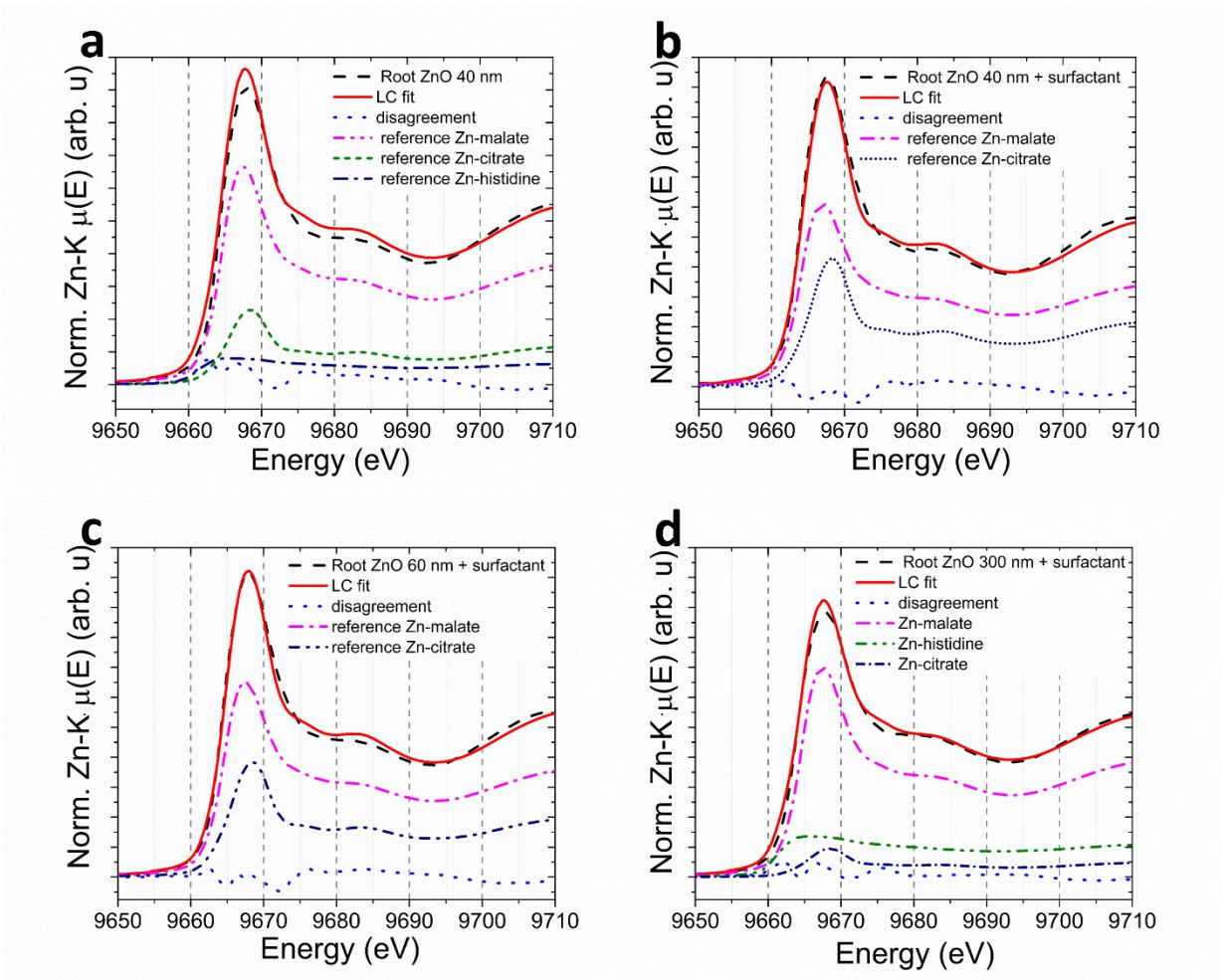

Fig. S13. Zn-K experimental XANES spectra recorded *in vivo* at root of bean (*Phaseolus vulgaris*) plants whose roots were immersed in nano ZnO dispersed in water: (a) 40 nm ZnO, (b) 40 nm ZnO + surfactant, (c) 60 nm ZnO + surfactant, and (d) 300 nm ZnO + surfactant.

Table S1. Characterization of ZnO nanoparticles. The table presents the putative size provided by the suppliers, crystallite size determined by XRD, nanoparticle diameter observed by SEM, hydrodynamic radius estimated by DLS, Zeta potential and Pearson's R from the adjusted slopes presented in Table 1. Due to features of the dispersions, it was not possible to measure the hydrodynamic radii for some dispersions.

Name in the manuscript	**Putative size (nm)**	**Supplier**	**Crystallite size (nm)**			**Diameter by SEM (nm)**	**Zeta potential (mv)**		**Z-average hydrodynamic radius (nm)**		**Pearson's R**	
			(100)	(002)	(101)		100 mg L^{-1}	1,000 mg L^{-1}	100 mg L^{-1}	1,000 mg L^{-1}	100 mg L^{-1}	1,000 mg L^{-1}
20 nm ZnO	20	M K Impex	14.0	14.5	13.8	23 ± 4	21±4	17±4	150±100	400±300	0.95	0.98
40 nm ZnO	40	M K Impex	25.6	47.1	26.0	32 ± 3	20±5	22±4	1,500±800	---------	0.98	0.99
60 nm ZnO	60	Nanophase	47.1	167.1	45.6	160 ± 30	28±5	27±3	500±300	---------	0.95	0.95
40 nm ZnO + surfactant	40	Nanophase	51.8	83.6	48.6	31 ± 8	-15±5	-10±5	90±30	90±50	0.83	0.96
60 nm ZnO + surfactant	60	Nanophase	68.1	63.4	62.2	67 ± 16	-16±5	-14±6	100±50	110±50	0.96	0.97
300 nm ZnO + surfactant	300	Agrichem	18.0	20.3	16.3	330 ± 40	-23±5	-41±7	----------	----------	0.91	0.87
$ZnSO4_{(aq)}$											0.95	0.99

$D_{(hkl)} = K \lambda / \beta \cos \theta$, where:

K, Scherrer constant (0.94 for spherical crystals);

λ, wavelength of the X-ray used for the diffraction (0.154184 nm);

β, integral breadth of the peak;

θ, angle of diffraction.

Table S2. Linear combination analysis of XANES spectra *in vivo* recorded at the stem and roots of bean (*Phaseolus vulgaris*) plants exposed to nano ZnO. Each spectrum corresponds to an average of three to five spectra.

Treatment	**Measured plant organ**	**Fraction (%)**				**Fit disagreement (%)**
		ZnO	Zn-Malate	Zn-Citrate	Zn-Histidine	
Pristine plant	Stem		95±2		5±2	0.56
ZnO 300 nm + surfactant	Stem		100			0.39
ZnO 60 nm + surfactant	Stem		100			0.43
ZnO 40 nm	Stem		67±4	33±4		0.36
ZnO 20 nm	Stem		84±2	16±2		0.26
ZnO 300 nm + surfactant	Root		71±4	8±5	21±2	0.50
ZnO 60 nm + surfactant	Root		66±4	34±4		0.33
ZnO 40 nm + surfactant	Root		62±6	38±7		0.46
ZnO 40 nm	Root		68±8	20±6	12±11	1.33
Unintentionally broken root ZnO 60 nm	Stem	74±2	27±2			0.34
Unintentionally broken root ZnO 40 nm	Stem	38±4	62±4			0.95
Intentionally cut root ZnO 300 nm + surf.	Stem	96±2	4±2			0.06
Intentionally cut root ZnO 20 nm	Stem	82±2	18±2			0.14

References

1. J. Peng, Y. Sun, Q. Liu, Y. Yang, J. Zhou, W. Feng, X. Zhang and F. Li, *Nano Research*, 2012, **5**, 770-782.
2. F. S. Hong, Z. G. Wei, Y. Tao, S. K. Wan, Y. T. Yang, X. D. Cao and G. W. Zhao, *Acta Botanica Sinica*, 1999, **41**, 851-854.